The Pennsylvania State University

The Graduate School

Department of Chemistry

STUDIES OF THE “INTRINSIC” FLUORESCENCE OF ROOM TEMPERATURE IONIC LIQUIDS

A Thesis in

Chemistry

by

Jing Hua Dong

Submitted in Partial Fulfillment
of the Requirements
for the Degree of

Master of Science

August 2007

Abstract

The "intrinsic" fluorescence of neat ionic liquids was studied in an attempt to identify its origin. The non-imidazolium ionic liquids (ILs), dimethyl(isopropyl)-propylammonium bis(trifluoromethylsulfonyl)imide, $[N_{ip311}^{+}][Tf_2N^{-}]$, and N-methyl-(N-propyl)pyrrolidinium bis(trifluoromethylsulfonyl)imide, $[Pr_{31}^{+}][Tf_2N^{-}]$, were studied using steady-state absorption, excitation, emission, and time-resolved emission spectroscopies. The emission spectra of both ILs showed similar excitation wavelength dependence as had been previously reported for imidazolium ionic liquids. Emission and excitation spectra and their behavior upon dilution demonstrate that the "intrinsic" fluorescence is actually due to impurities rather than being intrinsic to the IL. These impurities must occur as some related collection of chromophores. The estimated concentrations of chromophores absorbing at 400 nm is 3 ppm in $[N_{ip311}^{+}][Tf_2N^{-}]$ and 15 ppm in $[Pr_{31}^{+}][Tf_2N^{-}]$. The molar extinction coefficient of these chromophores was determined to be approximately 3000 cm^{-1} M^{-1}, which suggests some type of aromatic compounds.

TABLE OF CONTENTS

Introduction

Because most chemical reactions happen in solution, it is important to have the right solvent. But commonly used solvents are volatile organic compounds which pollute the environment due to their volatility. Much current research is being directed toward finding "green" alternatives to conventional solvents. Room temperature ionic liquids (RTILs) are one class of potential substitutes, mainly due to their nonvolatility. RTILs are defined as molten salts that are liquid below 100 ^{o}C[1]. Ionic liquids (ILs) have several unique physicochemical properties, such as very low vapor pressures, high ionic conductivities, and good chemical, thermal, and electrochemical stabilities[2,3]. These properties have led to intense research on ILs as potential organic and inorganic reaction media and as solvents for separation processes[2].

Most ILs consist of an organic cation and an inorganic anion[1]. Because there are many known cations and anions, the number of potential ILs is huge. This variety provides the hope that the properties of ILs can be tuned, making them "designer solvents" that can be specifically tailored for specific purposes. Because ILs are ionic conductors, their utilization as new electrolytes for electrochemical devices has also been the subject of intense study[4]. To support these applications many studies have also focused on different properties of RTILs. However research on the optical properties of RTILs has been limited.

To characterize some aspects of solvation in ILs, our group and others have measured absorption and emission spectra of dilute solutes. In these studies the ILs

themselves have been assumed to be transparent solvents much like conventional organic solvents. But ionic liquids are often slightly colored, and this color usually attributed to impurities. Very few studies have explored the nature of the absorption and emission of ILs themselves and thus far all such studies have been limited to imidazolium salts. All results to date show that ILs tend to absorb strongly below 300 nm. Samanta and coworkers have studied the problem most directly and have come to the conclusion that ILs possess intrinsic absorption and emission in the 300 – 400 nm region[5,6]. The present thesis describes further experiments designed to explore the possibility of intrinsic emission of ILs in this wavelength range.

Prior Studies of the Intrinsic Fluorescence of ILs

One of the first studies to consider the intrinsic absoption of ILs in relation to purification methods was performed by Billard et al.[7] These workers reported the importance of carefully purifying ionic liquids for optical work. With a purification procedure that combined treatment with activated charcoal and alumina, they reported that chloride impurities can be virtually eliminated, the sample made colorless to the eye, and the absorption band suppressed in the 250 – 300 nm range. Most IL synthesis involves alkyl chloride or bromine compounds to produce the desired cation. During the synthesis, water, halides, and chromophores (any kind of impurity that will cause the coloration of IL) may be retained in the end product, the IL. Some researchers have suggested that purification of the halide salt prior to metathesis would eliminate the chromophoric impurities. More recently, Earle et al.[8] advocated a

modified method for obtaining optically pure ionic liquids. These authors suggested that it is best to decolorize the final ionic liquid rather than the halide salt using a specially designed column. The column contains celite on the bottom, silica gel in the middle, and activated charcoal on the top. This method can be used as long as the IL does not contain a strongly hydrogen-bonding anion, or a cation that interacts with the carbon. After purification using this column, $[Im_{41}^{+}][PF_6^{-}]$ (Scheme 1) still has some weak absorption below 350 nm. The authors would call this absorption the "true" absorption of the IL. Still one could question whether the absorption remaining after purification is due to an impurity which is simply very hard to remove or whether it is actually intrinsic to the ionic liquid itself.

To date, the only workers to examine the optical properties of ILs in detail are Paul, Mandal, & Samanta, who published two papers[5,6] on the subject in 2005. In the first paper [5], these authors examined $[Im_{41}^{+}][PF_6^{-}]$. $[Im_{41}^{+}][PF_6^{-}]$ was prepared by dropwise addition of ice-cooled HPF_6 (65% solution in water) to an ice-cooled aqueous solution of $[Im_{41}^{+}][Cl^{-}]$. After the reaction mixture was stirred for 24 h at room temperature, the upper acidic layer was removed. Then the ionic liquid portion was washed with water multiple times until pH paper showed no acidity. At the same time, the wash water and ionic liquid were tested with $AgNO_3$ solution for any halide impurities. The $[Im_{41}^{+}][PF_6^{-}]$ was then mixed with activated charcoal and filtered several times through a celite column and finally dried in a vacuum oven to remove any volatile organic impurities or water. The water content of the IL sample was less than 100 ppm. Although the IL was stored in a desiccator under nitrogen,

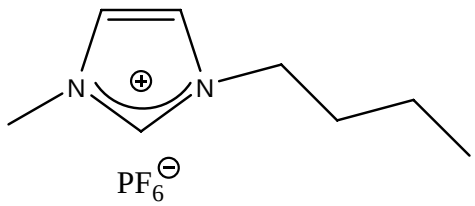

Scheme 1: 1-methyl-3-butylimidazolium hexafluorophosphate, $[Im_{41}^{+}][PF_6^{-}]$.

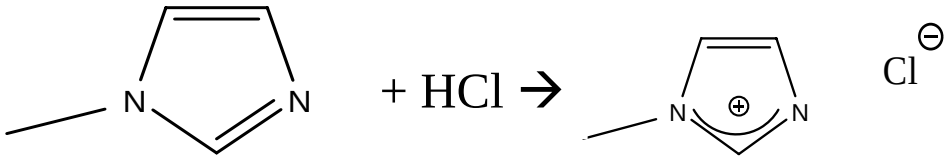

Scheme 2: Protonation of 1-methylimidazole (MIM) with HCl to produce $[Im_{10}^{+}][Cl^{-}]$.

the steady state experiments were run with freshly prepared ionic liquid to avoid any contamination.

Even with this highly pure sample, Paul et al. showed that $[Im_{41}^{+}][PF_6^{-}]$ has strong absorption at 280 nm and possesses a long-wavelength tail that extends beyond 300 nm. They noted that the observed OD of ~0.1 at 350 nm means that more than 20% of the incident light is absorbed by the IL at this wavelength. Given that the imidazolium cation is an aromatic compound, it is not surprising that it would show absorption in the UV/Visible region. To demonstrate that the absorption is not due to an impurity, protonation of MIM (1-methylimidazole) (Scheme 2) with HCl was studied. Addition of acid to MIM, which has an absorption maximum at 280 nm, produced a new species which absorbed at 330 nm, similar to what is formed in $[Im_{41}^{+}][Cl^{-}]$. Proof that no third species exists in the sample was provided by the presence of an isosbestic point at 285 nm. Through this experiment, the Paul et al. demonstrated that the imidazolium cation does absorb at 280 nm and this absorption does extend beyond 300 nm.

Paul and Samanta also examined the fluorescence of $[Im_{41}^{+}][PF_6^{-}]$. Emission spectra obtained when the sample was excited below 300 nm revealed two emission bands, one at 337 nm and another at 410 nm (Fig. 1). As the excitation wavelength was increased, the shorter wavelength component decreased in intensity and then disappeared. At the same time, the longer wavelength component became more and more prominent, and its frequency shifted to the red as the excitation wavelength increased. As a control experiment, emission spectra of MIM and HCl were also

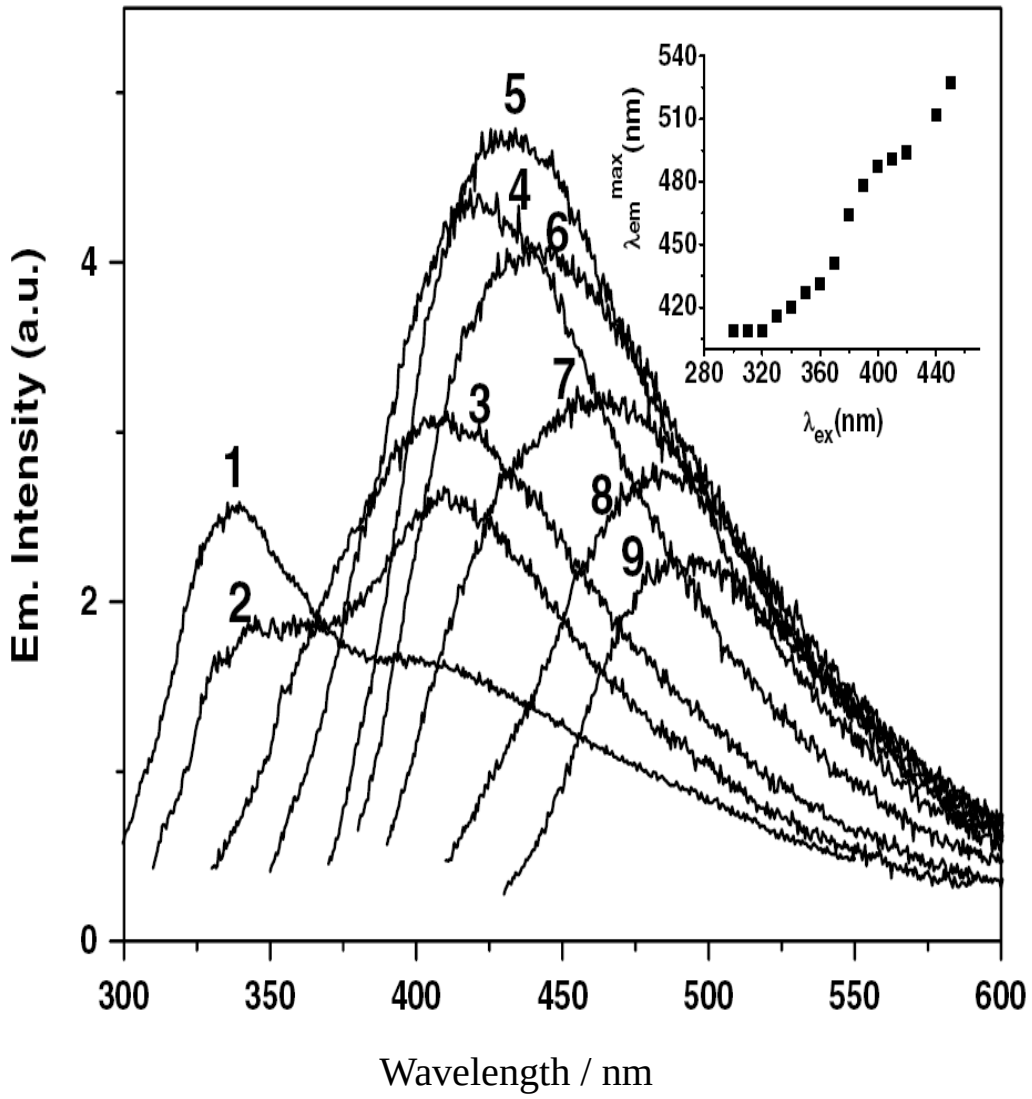

Fig. 1: Excitation wavelength dependent fluorescence spectra of $[Im_{41}^{+}][PF_6^{-}]$ [5]. λ_{exc} values are 280 (1), 300 (2), 320 (3), 340 (4), 360 (5), 370 (6), 380 (7), 400 (8), and 420 (9) nm. A license agreement (License number: 1816560932224) was obtained from the Elsevier.

recorded and two components were again observed. This observation led the authors to conclude that the short wavelength component is due to the imidazolium monomer and suggest that the long wavelength component is due to differently associated species in the sample.

Further support for these ideas was provided in a second paper[6] in which Paul et al. examined the absorption and the emission of the related ILs $[Im_{21}^{+}][BF_4]$, $[Im_{41}^{+}][BF_4^{-}]$, and $[Im_{41}^{+}][Cl^{-}]$. The absorption spectra of these imidazolium ILs showed significant absorbance (0.007 – 0.15) even at 350 nm and a long visible tail extending beyond 400 nm. Similar trends were observed with these ILs as with $[Im_{41}^{+}][PF_6^{-}]$. For example, when these ILs were excited at or below 300 nm, two components were observed in the emission. As the excitation wavelength was shifted toward redder wavelengths, the shorter wavelength component of the emission decreased in intensity and the longer wavelength component become dominant. Due to the presence of two components and the shifting of the emission spectra, the quantum yield of the neat ionic liquids is not well defined. But the authors did estimate the emission quantum yields of these neat ionic liquids to be between 0.005 and 0.02 at 360 nm excitation. From the time-resolved fluorescence decay experiments, they observed the major component to have a time constant of 470 – 590 ps.

Because all the ionic liquids exhibit the similar behavior, Paul et al. wanted to find out what is causing the increase in intensity for the longer-wavelength component and its shift with excitation wavelength. The long absorption tail might indicate that

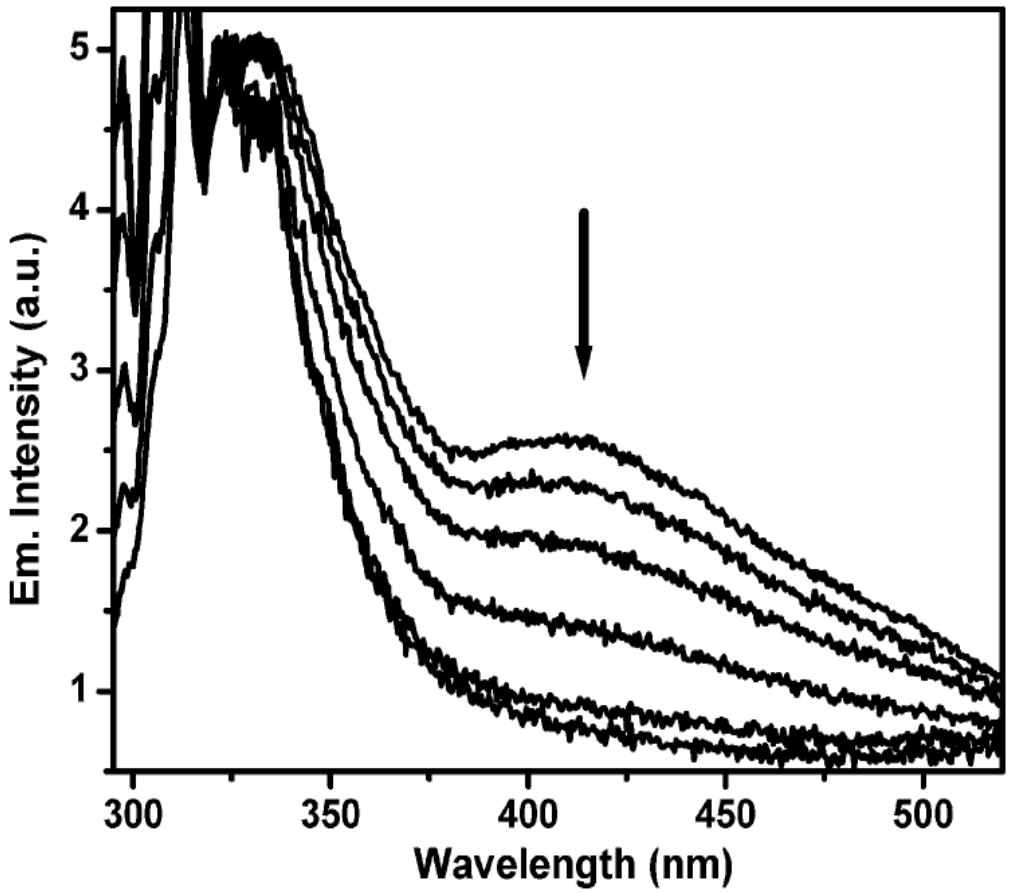

Fig. 2: Effect of dilution with acetonitrile on the fluorescence profile of $[Im_{41}^{+}][PF_6^{-}]$, λ_{ex} = 285nm. The spectra are normalized at the lower wavelength emission maximum. The arrow indicates that the band decreases with decreasing concentration. Concentration are 0.35, 0.15, 0.07, 0.03, 0.007, and 0.0015 M[6]. Permission was granted by the American Chemical Society.

various differently associated species exist within the sample. To examine this possibility, the effect of dilution by acetonitrile was studied. Emission spectra (λ_{ex} = 285 nm) were recorded at different concentrations of $[Im_{41}^{+}][PF_6^{-}]$ in acetonitrile (Fig. 2). As mentioned previously, two components were observed when the IL was excited at blue wavelengths. In Fig. 2, the spectra were normalized to the emission maximum of the short wavelength component. As the concentration of the ionic liquid decreased, the long wavelength emission band decreased relative to the short wavelength band and eventually disappeared. This observation lead Paul et al. to suggest that the long tail in the absorption spectrum of imidazolium ILs is due to the presence of a collection of differently associated species, each with its own unique energy levels. When the sample is excited at different wavelengths, different species are excited and their emission characteristics observed. The decrease and disappearance of the long wavelength emission band was interpreted in terms of that these associated species are breaking up upon dilution in acetonitrile.

Two very recent papers relate to the observations of Paul et al. In a 2007 paper[9] Burrell et al. claimed that there should be no intrinsic fluorescence in ionic liquids. They asserted at whatever emission is observed must be due to residual impurities, but they did little to establish this claim or directly refute the findings of Paul et al. In a spectroscopic study primarily focused on solute spectroscopy, Gutowski et al. [10] reported excitation wavelength dependent emission of neat $[Im_{41}^{+}][BF_4^{-}]$ very similar to that of Paul et al. These authors also measured steady-state emission anisotropies as a function of temperature. They analyzed their data in terms of the Perrin equation,

$$\frac{1}{r_{IL}} = \frac{1}{r_0} + \frac{\tau}{r_0 V_{IL}} . \frac{kT}{\eta} \qquad (1)$$

where r_{IL} is steady state anisotropy, r_0 is the initial anisotropy, τ is the lifetime, V_{IL} is the hydrodynamic volume, and η is the viscosity of the IL, and kT is Boltzmann's constant multiplied by the temperature. The intercept of a plot of $\frac{1}{r_{IL}}$ versus $\frac{T}{\eta}$ provided an initial anisotropy of 0.29 ± 0.01, and the slope provided a hydrodynamic volume of the emitting species of 780 ± 40 Å^3. The van der Waals volume of an $[Im_{41}^+][BF_4^-]$ ion pair is 198 Å^3. Because there is great difference between this hydrodynamic volume and the van der Waals volume, one can conclude that some entity larger than a single $[Im_{41}^+]$ cation or an $[Im_{41}^+][BF_4^-]$ ion pair is the chromophoric species being observed.

The Maroncelli group has undertaken a number of studies of solute spectroscopy in ILs [11-16]. During the course of this work we have measured the absorption and emission spectra of a number of neat ILs and have observed behavior of the sort described by Paul and Samanta, even in the absence of the aromatic imidazolium cation. The purpose of the present thesis is to provide a more systematic study of non-imidazolium ILs in order to examine whether intrinsic fluorescence might be a feature common to all ionic liquids.

Experimental

1. Materials

The ionic liquids selected for this study are dimethyl(isopropyl)propylammonium bis(trifluoromethylsulfonyl)imide, $[N_{ip311}^{+}][Tf_2N^{-}]$ and N-methyl(N-propyl)pyrrolidinium bis(trifluoromethylsulfonyl)imide $[Pr_{31}^{+}][Tf_2N^{-}]$ (Scheme 3). These ILs were synthesized by Gary A. Baker of the Chemical Science Division, Oak Ridge National Laboratory. They were chosen for this work because they are spectroscopically the cleanest ones in our RTIL collection. The ILs were initially used as received. Later, both samples were treated with active charcoal and filtered through a syringe filter with 0.22 μm filter paper. $[Nip_{311}^{+}][Tf_2N^{-}]$ has a water content of 530 ppm and a viscosity of 104.6 cP at 25°C. The water content of $[Pr_{31}^{+}][Tf_2N^{-}]$ is 61 ppm, and its viscosity is 51.5 cP at 25°C. Because ILs absorb water from the atmosphere, samples were stored in a nitrogen-purged glove box. The ILs were transferred from their original container (received from Baker) into 1 cm quartz cuvettes in the glove box and sealed with parafilm for spectroscopic work.

2. Instrumentation

Steady-state absorption spectra were obtained using a Hitachi U-3000 UV/Vis spectrophotometer. Fluorescence spectra were measured using a Spex Fluorolog F212 fluorimeter and were corrected for emission responsivity. The resolution used

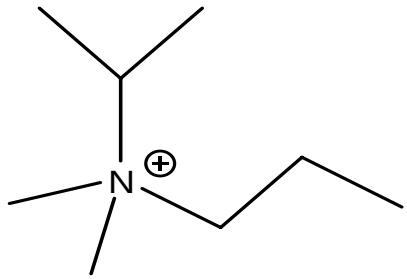

[N_{ip311}^{+}]

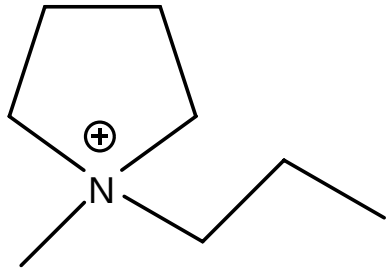

[Pr_{31}^{+}]

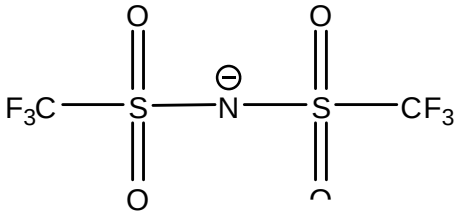

[Tf_2N^{-}]

Scheme 3: Structures of dimethyl(isopropyl)propylammonium bis(trifluoromethylsulfonyl)imide, [Nip_{311}^{+}][Tf_2N^{-}] and N-methyl(N-propyl)pyrrolidinium bis(trifluoromethylsulfonyl)imide [Pr_{31}^{+}][Tf_2N^{-}].

for absorption and emission were 1.0 and 1.7 nm respectively. Time-resolved emission measurements were made using a home-build time-correlated single photon counting system. As the excitation source, the doubled output of a mode-locked fs Ti:sapphire laser (Coherent Mira 900F) was used (λ_{ex} = 400 nm). Emission from the sample was collected through a single monochromator (ISA H10) with an 8-nm band pass, over time ranges of 3 – 10 ns, depending on the lifetime of the sample. The FWHM of the instrument function was estimated to be about 25 ps by measuring the response to a scattering solution. Emission decays were fit together with instrument response functions using an iterative reconvolution least-squares algorithm which enhances the effective time resolution to ~10 ps[17].

Results

1. Absorption

The Maroncelli group has measured the absorption spectra of many different ILs (Fig. 3). In all cases some structure is observed which is probably caused by specific impurities. However, in addition, all of the ILs including $[N_{ip311}^{+}][Tf_2N^{-}]$ and $[Pr_{31}^{+}][Tf_2N^{-}]$ show absorption well beyond 300 nm. For $[Pr_{31}^{+}][Tf_2N^{-}]$, the spectrum shown here has been referenced to the cyclohexane absorption spectrum in order to correct for cuvette absorption and scattering ($[Pr_{31}^{+}][Tf_2N^{-}]$ and cyclohexane have very similar refractive indices). After correction, the $[Pr_{31}^{+}][Tf_2N^{-}]$ absorption spectrum still shows an optical density of 0.11 at 350 nm, which means that 22% of the incident light is absorbed by the IL at this wavelength. Also, all of the spectra shown in Fig. 3 have a long tail which is similar to what is observed in the imidazolium ILs studied previously [6]. Based on Fig. 3 it appears that even in the absence of an obvious chromophore such as Im_{41}^{+}, ILs show a long absorption tail that extends well beyond 300 nm.

2. Excitation Dependence of Emission

Previous papers[5,6,10] demonstrated that the fluorescence of imidazolium ionic liquids has a strong excitation wavelength dependence. To confirm this behavior in other classes of ILs, both $[N_{ip311}^{+}][Tf_2N^{-}]$ and $[Pr_{31}^{+}][Tf_2N^{-}]$ were excited at various wavelengths. $[N_{ip311}^{+}][Tf_2N^{-}]$ was excited at different wavelengths in the region of

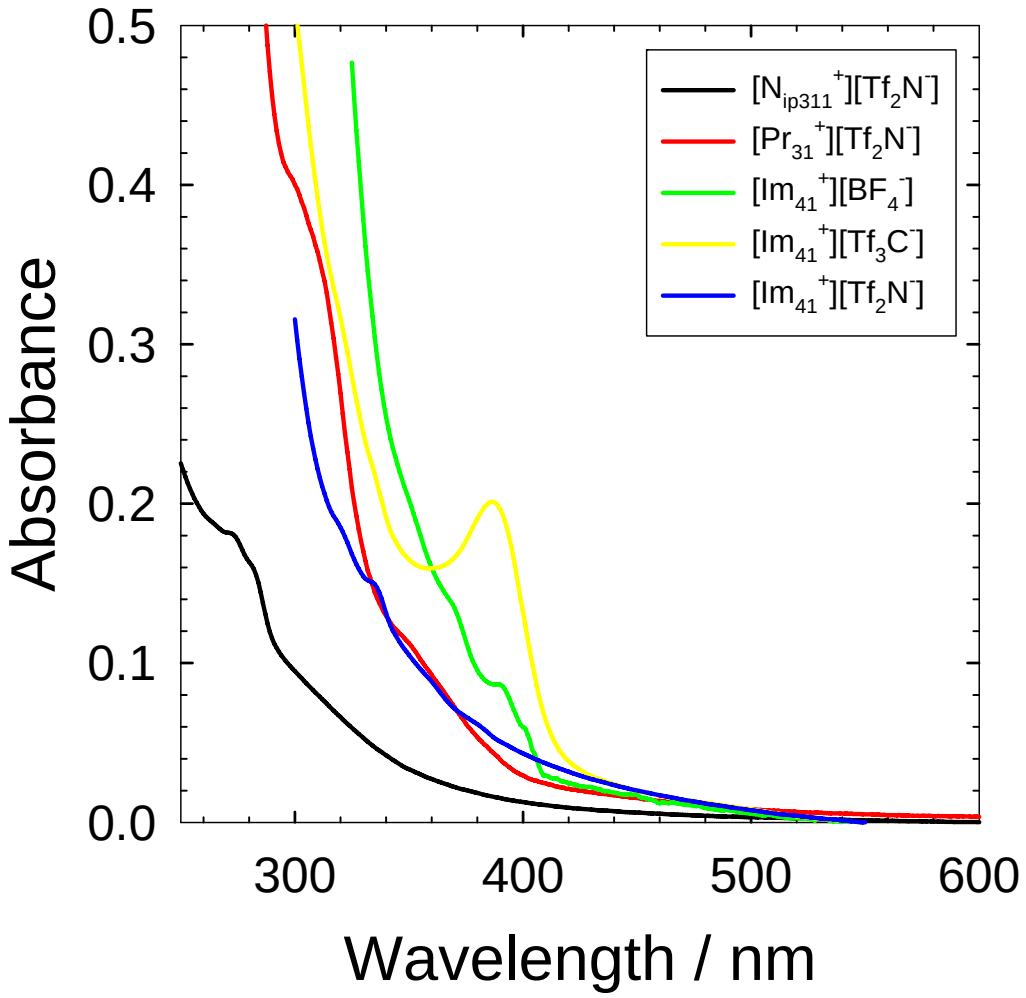

Fig. 3: Absorption spectra of various ionic liquids at 25°C.

250 – 460 nm (Fig. 4). When the sample is excited at wavelengths lower than 320 nm, two peaks were observed in the spectra, a sharp peak at 330 nm and a broader peak at longer wavelengths (about 395 nm). As the excitation wavelength is increased beyond 320 nm, the shorter wavelength component disappears. At λ_{ex} = 320 nm, only the longer wavelength peak can be observed. As the excitation wavelength is shifted toward longer wavelengths, the intensity of the peak decreases and its position red shifts.

Many papers described the use of activated charcoal to improve the optical purity of ionic liquids. This method was used with $[N_{ip311}^{+}][Tf_2N^{-}]$ to reduce the impurity in the sample. The absorption spectra of untreated and treated $[N_{ip311}^{+}][Tf_2N^{-}]$ samples are shown in Fig. 5. The absorbance at wavelengths below 300 nm is suppressed, but more absorbance is present at wavelengths beyond 300 nm. When the treated $[N_{ip311}^{+}][Tf_2N^{-}]$ sample was excited at the same wavelengths shown in Fig. 4, the emission spectra shown in Fig. 6 were obtained. The overall intensity of the spectra is decreased slightly compared to the untreated sample. For example, the intensity of peak of the untreated sample when excited at 360 nm is about 3500 counts/s and the intensity of the treated sample when excited at same wavelength is about 2700 counts/s. In addition, when the treated sample is excited below 320 nm, the shorter wavelength component is suppressed compared to the data in Fig. 4. Unlike the case of imidazolium ionic liquids where one expects a low wavelength band due to the aromatic cation, a strong bond is not expressed here. We suspect that this band disappears because it is due to some impurity. Emission spectra

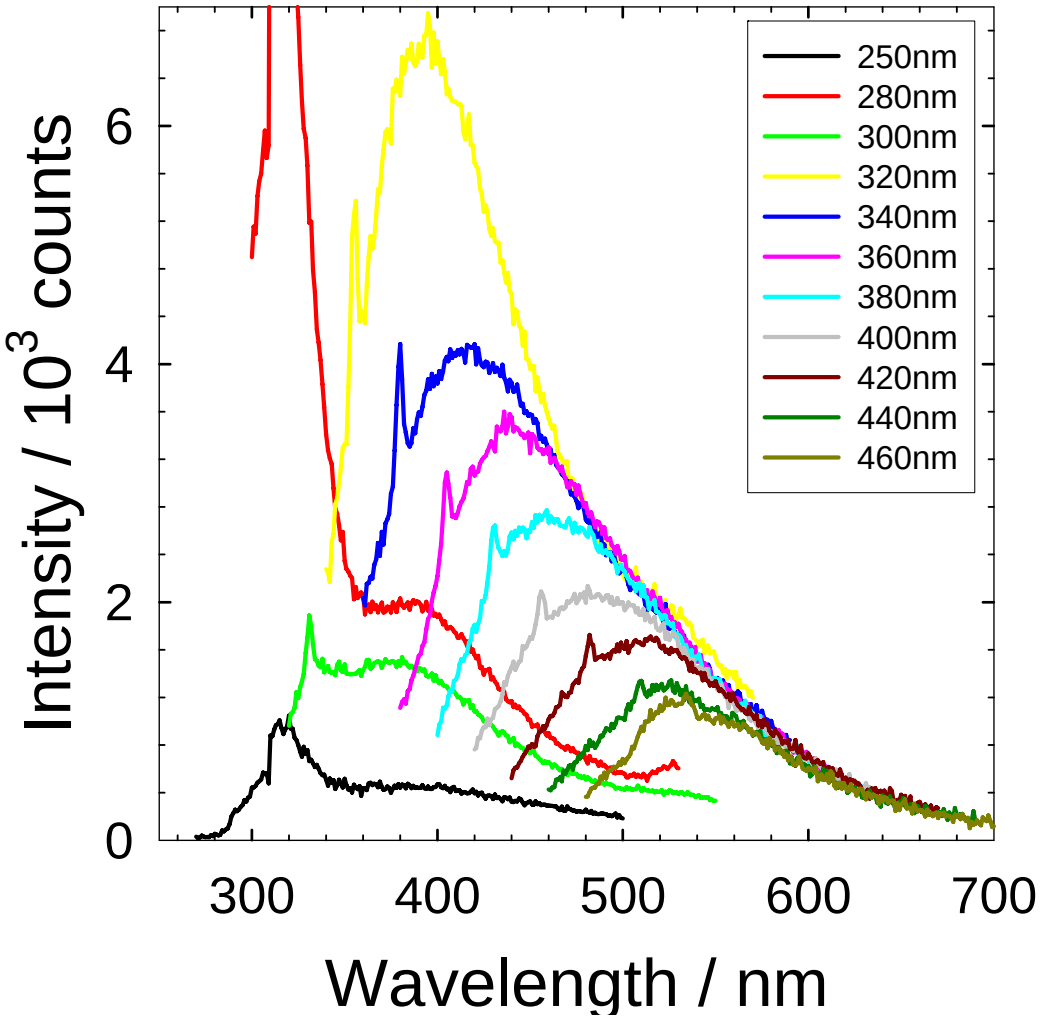

Fig. 4: Emission spectra of $[N_{ip311}^{+}][Tf_2N^{-}]$ excited at various wavelengths. The small sharp peak in each spectrum is due to Raman scattering.

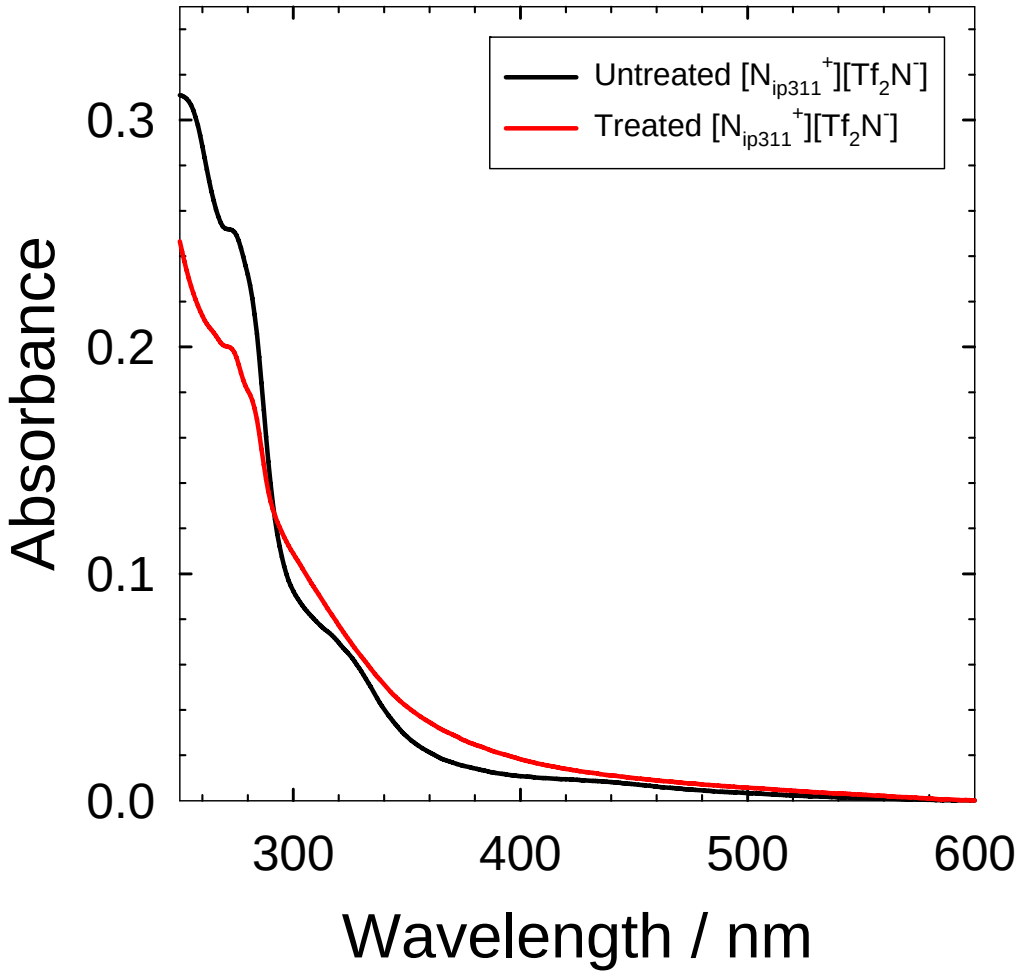

Fig. 5: Absorption spectra of [N_{ip311}^{+}][Tf_2N^-] before and after treatment with active charcoal.

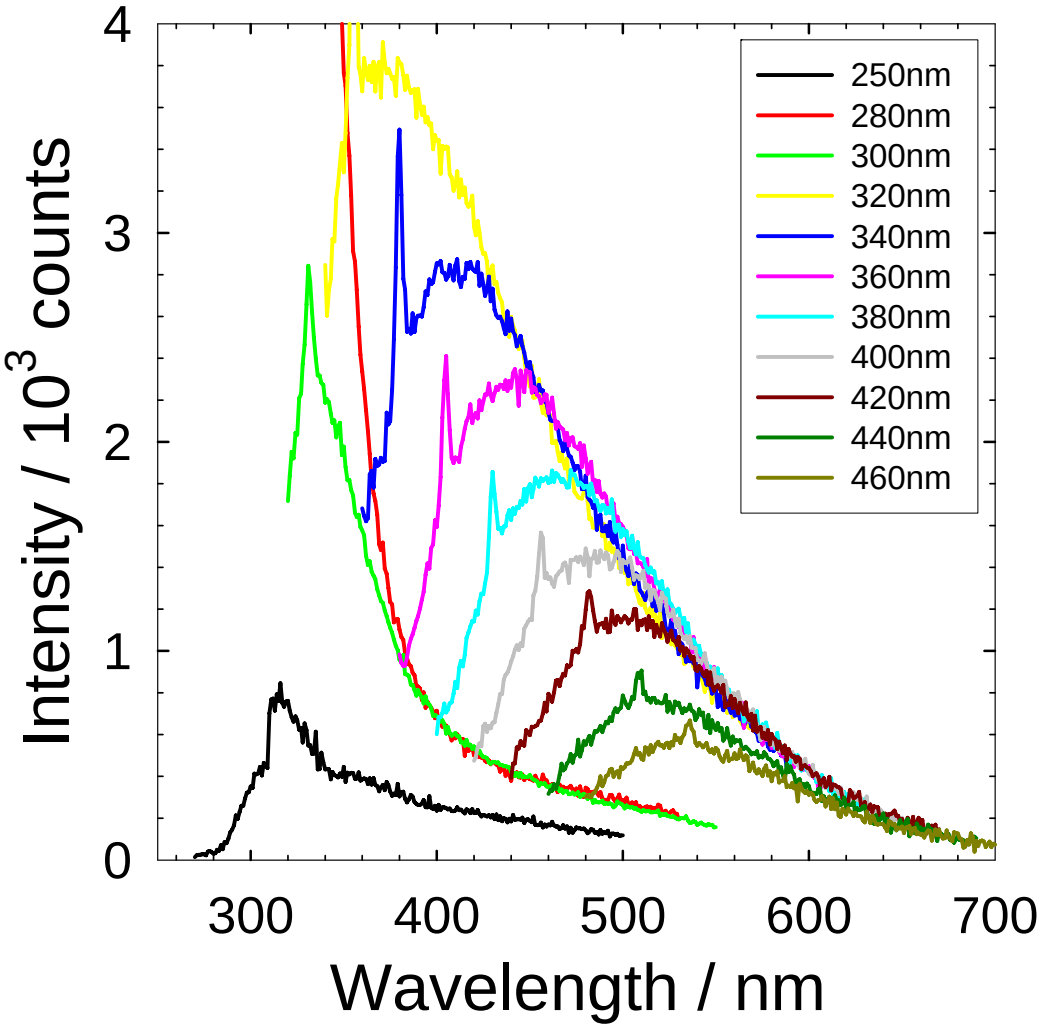

Fig. 6: Emission spectra of $[N_{ip311}^{+}][Tf_2N^{-}]$ treated with active charcoal excited at various wavelengths.

excited beyond 320 nm experience the same trend as in the untreated sample, but the intensity of the emission is decreased slightly.

Fig. 7 shows $[Pr_{31}^{+}][Tf_2N^{-}]$ when excited in the range of 250 – 500 nm. The excitation wavelength dependence observed here is similar to that of $[N_{ip311}^{+}][Tf_2N^{-}]$. Two components are observed in the spectra when excited below 320 nm. As the excitation wavelength is increased, a longer wavelength component becomes dominant. Also, the position of the long wavelength peak is shifted to longer wavelengths while its intensity goes through a maximum at an excitation wavelength of 340 nm. When the sample is excited between 320 – 360 nm, the emission is much more intense than at other excitation wavelengths, which suggests that some kind of molecular impurity is being excited. Also, the emission intensity is approximately 10-fold higher in $[Pr_{31}^{+}][Tf_2N^{-}]$ than in $[N_{ip311}^{+}][Tf_2N^{-}]$. The absorption spectra in Fig. 3 show that the absorption of $[Pr_{31}^{+}][Tf_2N^{-}]$ is much higher than that of $[N_{ip311}^{+}][Tf_2N^{-}]$, so this greater emission of $[Pr_{31}^{+}][Tf_2N^{-}]$ is expected.

Fig. 8 shows a plot of the peak frequency of the long wavelength component band as a function of excitation frequency for a variety of different ionic liquids. Data on $[N_{ip311}^{+}][Tf_2N^{-}]$ and $[Pr_{31}^{+}][Tf_2N^{-}]$ as well as literature data[5,6,10] are included for comparison. At the longer excitation wavelengths (lower frequencies); all of the data are similar to one another. But when the sample is excited at bluer wavelengths, the agreement is lost. We believe that this divergent behavior at higher frequencies is due to the fact that excitation of impurities is unavoidable for frequencies greater than 31000 cm^{-1}. Both sets of $[Im_{41}^{+}][BF_4^{-}]$ data from two different groups show

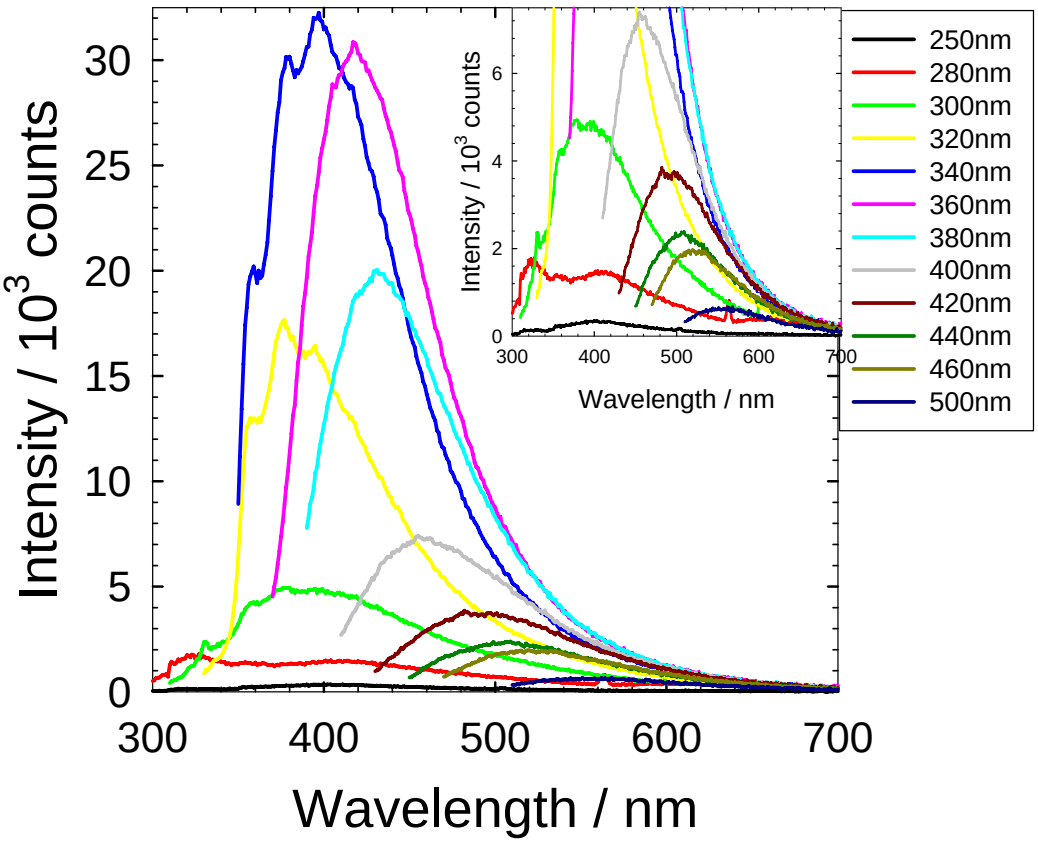

Fig. 7: Emission spectra of $[Pr_{31}^{+}][Tf_2N^{-}]$ excited at various wavelengths. The small sharp peak on the spectrum is due to Raman scattering. The insert shows the lower portion of the spectra for clearer view of the spectral shift.

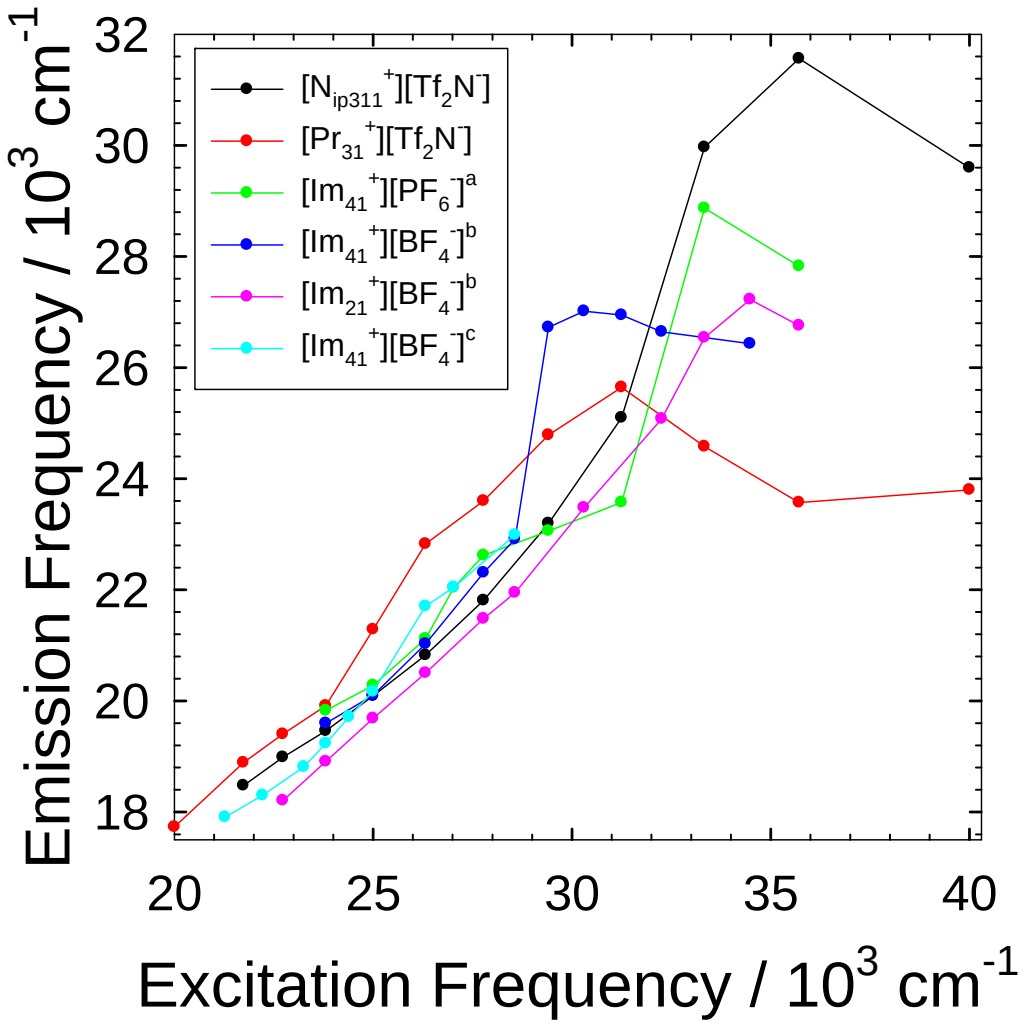

Fig. 8: Peak emission frequencies as function of excitation frequencies in various ionic liquids, a is data from Ref. 5, b from Ref. 6, and c from Ref. 10.

very similar results. Even with different ionic liquids, all of the peak frequencies shift with excitation wavelength in a nearly identical monomer, which suggests that the red shift behavior might be is common to all ionic liquids.

In addition to emission spectra, a few excitation spectra were measured for both $[N_{ip311}^{+}][Tf_2N^{-}]$ and $[Pr_{31}^{+}][Tf_2N^{-}]$. If the sample contains only one species, then the excitation spectrum should be same as the absorption spectrum. If there is more than one species present, the excitation spectrum may or may not be same as the absorption spectrum. If the shape of the band or the peak position is different when the excitation spectra are monitored at different emission wavelengths, then there are multiple species in the sample. Emission spectra were obtained by exciting at 360, 400, and 440 nm for both $[N_{ip311}^{+}][Tf_2N^{-}]$ and $[Pr_{31}^{+}][Tf_2N^{-}]$, and excitation spectra were taken by setting the monitoring wavelength to be the peak of the emission spectrum at each of these three excitation wavelengths (Figs. 9 and 10). Excitation spectra shift similarly to the emission spectra. The excitation spectra of $[Pr_{31}^{+}][Tf_2N^{-}]$ are more structured than those of $[N_{ip311}^{+}][Tf_2N^{-}]$. Note for example, the shoulder on the 440 nm spectrum and the two peaks appearing in the 360 nm spectrum.

The large range of emission frequencies in the emission spectra indicates a broad distribution of absorbing and emitting species. The evidence from emission shows that there are different sub-ensembles within the sample, which means that there is some source of heterogeneity in IL. The observation of shifting in the excitation spectra also suggests the presence of many species in the ILs. The emission of

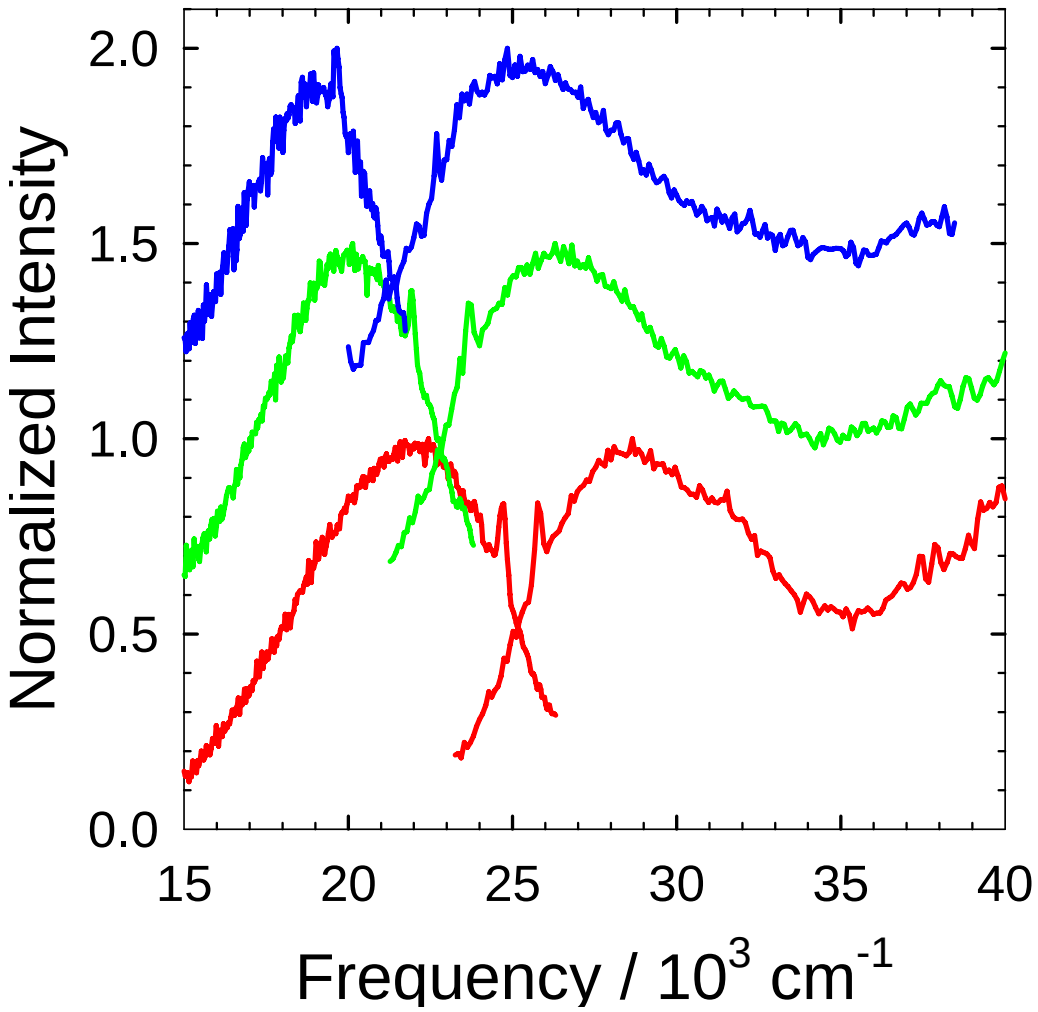

Fig. 9: Emission and excitation spectral pairs of $[N_{ip311}^{+}][Tf_2N^{-}]$, λ_{ex} = 360 (red), 400 (green), and 440 nm (blue). Monitored emission wavelengths for λ_{ex} = 360, 400, and 440 nm are 440, 485, and 510 nm. The spectra excited at 400 nm are vertically shifted by 0.5 and the spectra at λ_{ex} = 440 nm are shifted by 1.0 for charity.

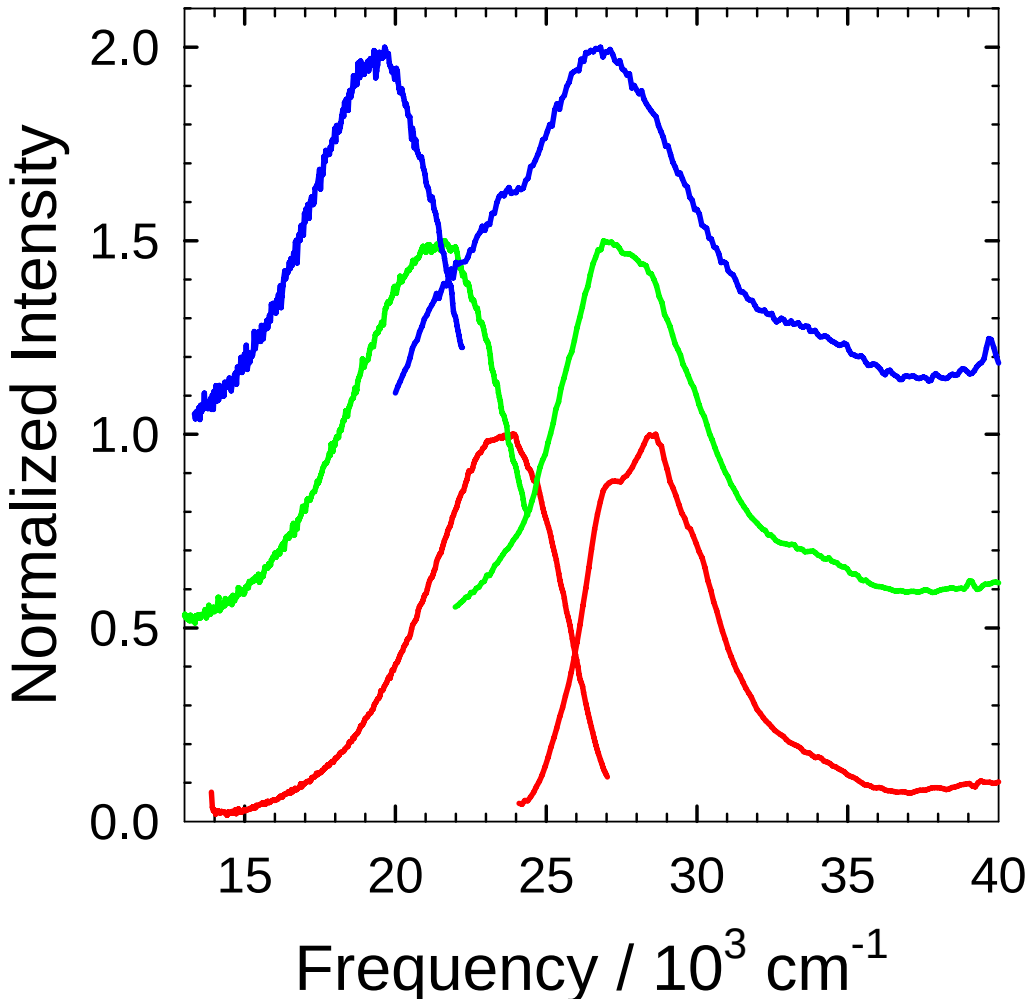

Fig. 10: Emission and Excitation spectra pairs of $[Pr_{31}^{+}][Tf_2N^{-}]$, λ_{ex} = 360 (red), 400 (green), and 440 nm (blue). Monitored emission wavelengths for λ_{ex} = 360, 400, and 440 nm are 419, 460, and 507 nm. The spectra excited at 400 nm are vertically shifted by 0.5 and the spectra at λ_{ex} = 440 nm are shifted by 1.0 for charity.

$[N_{ip311}^{+}][Tf_2N^{-}]$ experiences a 3000 cm^{-1} shift when excited between 360 nm and 440 nm; and the emission of $[Pr_{31}^{+}][Tf_2N^{-}]$ has a 1500 cm^{-1} shift. Both shifts are too large to be due to only to environmental effects. They must instead result from the presence of a distribution of distinct absorbing and emitting chromphores.

Samanta and coworkers[5,6] suggest that the long absorption band of ILs is due to $[Im_{41}^{+}]$ chromophores in different states of aggregation. When the excitation wavelength is changed, different associated species are excited.

3. Emission Decays

Fluorescence time-resolved measurements can yield the lifetime of the emitting species in a sample, which is needed in the next section. Also, one can tell whether the sample is heterogeneous or not. Fig. 11 shows representative fluorescence decays of $[N_{ip311}^{+}][Tf_2N^{-}]$ at different emission wavelengths (440, 490, and 550 nm) when it is excited at 400 nm. For comparison purposes, all three decay are normalized. Overall, more than 20 decays were measured, and all of these decays are similar to those plotted in Fig. 11. The particular emission wavelengths in Fig. 11 were chosen according to the steady-state emission spectrum; the emission spectrum peaks at 490 nm; 440 and 550 nm are the half intensity points of the spectrum. For each monitored wavelength, parallel, magic, and perpendicular angles were recorded. We also measured fluorescence decays of $[Pr_{31}^{+}][Tf_2N^{-}]$ in a similar way (Fig. 12). The fluorescence decays are best fit by a tri-exponential function with a main component (50%) having a time constant of 50 – 95 ps, an intermediate

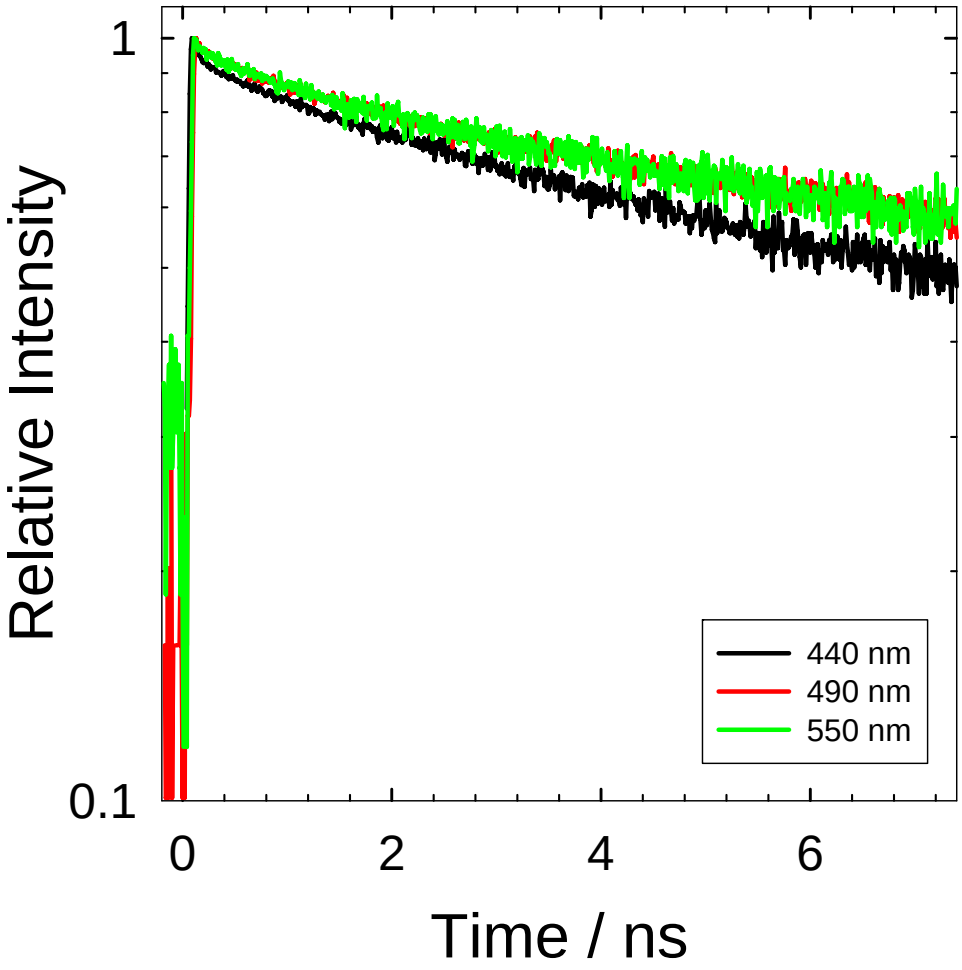

Fig. 11: Fluorescence decays of $[N_{ip311}^{+}][Tf_2N^{-}]$ monitored at 440, 490, 550 nm when excited at 400 nm.

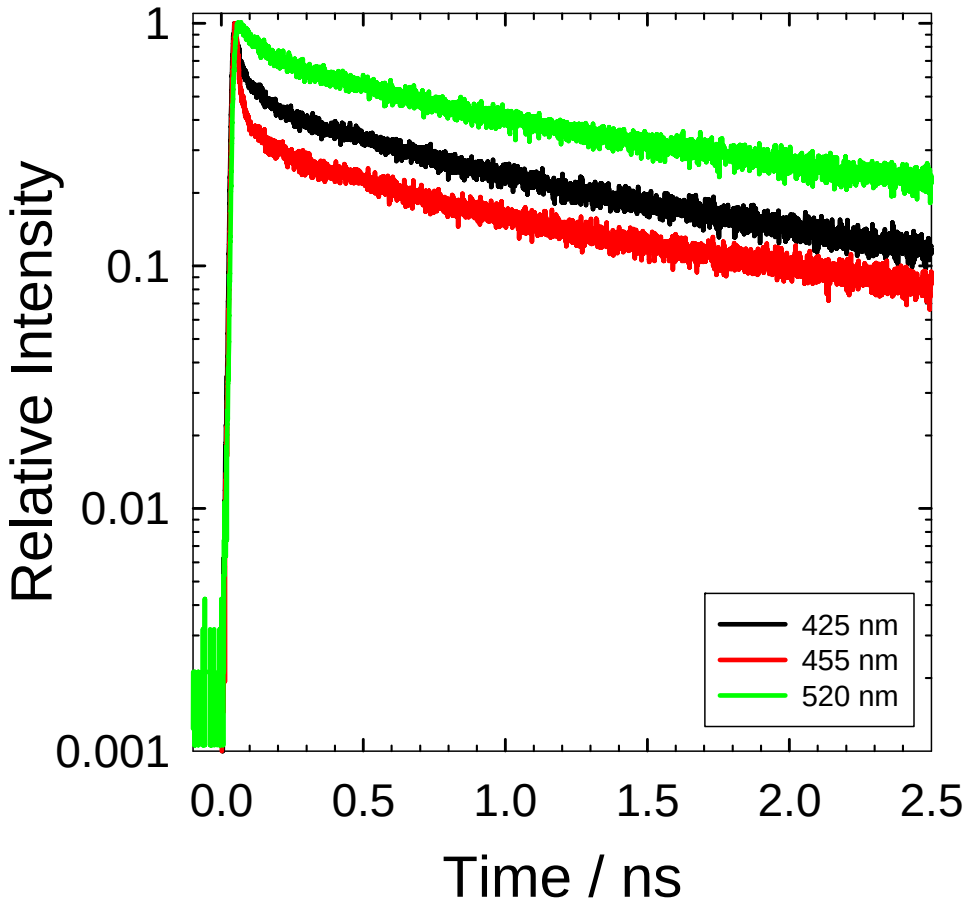

Fig. 12: Fluorescence decays of $[Pr_{31}^{+}][Tf_2N^{-}]$ monitored at 425, 455, 520 nm when excited at 400 nm.

component (30%) having a time constant of 735 – 840 ps, and a third component (20%) with a time constant of 3 – 4 ns. Some of the decays also have a very fast component (< 10 ps) which is due to Raman scattering. Beside this fastest component, $[Pr_{31}^{+}][Tf_2N^{-}]$ was fitted to tri-exponential function with 42 % of 100 - 200 ps, 36 % of 1.0 – 1.2 ns, and 22 % of 4.0 – 5.5 ns.

4. Approximate Quantum Yield and Concentration Determinations

The purpose of this paper is to discover the origin of the fluorescence of ILs, and for this purpose it might be useful to know the concentration of the fluorophores. To do so we assume there are two "important" electronic states, a ground and a single electronically excited state, so that Strickler-Berg relationship[18] between the radiative decay rate and absorption strength is valid. The general assumptions for validity of the Strickler-Berg relationship are that 1) there are no changes in refractive index between the absorption and emission wavelengths, and 2) there is no geometry change in the excited-state, which is the main assumption. The Strickler-Berg relationship can be written:

$$k_r = 2.88 \times 10^{-9} n^2 \left\langle \upsilon^{-3} \right\rangle^{-1} \int \frac{\varepsilon(\upsilon) d\upsilon}{\upsilon} \qquad (2)$$

where k_r is the radiative decay rate constant, n is the refractive index of the medium, $\left\langle \upsilon^{-3} \right\rangle = \frac{\int F(\upsilon) d\upsilon}{\int F(\upsilon) \upsilon^{-3} d\upsilon}$ with $F(\upsilon)$ denoting the observed emission spectrum, and $\varepsilon(\upsilon)$ the absorption spectrum in terms of the molar extinction coefficient.

If we know $\varepsilon(\upsilon)$, the concentration of fluorophore can be directly estimated from the observed absorption spectrum. $\varepsilon(\upsilon)$ can be obtained from the Strickler-Berg

relation if k_r is measured independently, which can be done with the quantum yield Q and the lifetime τ of the fluorophore measured in the previous section:

$$k_r = \frac{Q}{\tau} \tag{3}$$

$$k_{nr} = \frac{1}{\tau} - k_r \tag{4}$$

Once radiative decay rate constant is known, the nonradiative decay rate constant k_{nr} can also be calculated from k_r using Eq (4).

The fluorescence quantum yield Q is the ratio of the number of photons emitted to the number of photons absorbed. The closer the quantum yield of a fluorophore is to unity, the brighter is its emission. To estimate the quantum yield the emission of a fluorophore can be compared to the emission of some standard having a known quantum yield, using the relation

$$Q = \frac{n_R^2 I_S \left(1 - 10^{-A_R}\right)}{n_S^2 I_R \left(1 - 10^{-A_S}\right)} Q_R \tag{5}$$

where n_X is the refractive index, I_x is the integrated emission intensity, and A_X is the absorbance of the sample (X=S) and reference (X=R) solutions. In the present study, a solution of C153 in methanol was used as the standard (Q_R = 0.42)[19]. Fluorescence quantum yields of $[N_{ip311}^+][Tf_2N^-]$ and $[Pr_{31}^+][Tf_2N^-]$ were determined using equation (5).

Table 1 summarizes all of the parameters needed to calculate quantum yields at three different excitation wavelengths, 360, 400, and 440 nm. For $[N_{ip311}^+][Tf_2N^-]$, we find that the quantum yield is 1.8 x 10^{-2} at λ_{ex} = 360 nm. Samanta and coworkers[6] previously estimated quantum yields in neat imidazolium ionic liquids to be in the range 0.005 to 0.02 at λ_{ex} = 360 nm, which is similar to the results obtained here.

The final quantity needed to estimate the fluorophore concentration is the fluorescence lifetime, which specifies the average amount of time a molecule spends in the excited state before returning to the ground state. The emission decays from the previous section were fit to triple exponential functions and the lifetimes τ calculated by

$$\tau = \sum_i a_i \tau_i \tag{6}$$

where a_i is the fractional amplitude of each component i, and τ_i is its time constant. The lifetime used in the calculation of k_r is the average value over all emission wavelengths that were measured. The average lifetime of $[N_{ip311}^+][Tf_2N^-]$ excited at 400 nm is 1.0 ns. We assume that it is the same at other excitation wavelengths.

The integral in Eq (2), which is related to the concentration desired, can be expressed in terms of k_r as follows

$$\int \frac{\varepsilon(\upsilon) d\upsilon}{\upsilon} = \frac{k_r}{2.88 \times 10^{-9} n^2 \langle \upsilon^{-3} \rangle^{-1}}.$$

According to Beer's Law, the molar extinction coefficient is given by $\varepsilon(\upsilon) = \frac{A(\upsilon)}{c \cdot l}$, where $A(\upsilon)$ is the absorbance at a certain frequency υ, c is the concentration, and l is the path length. This relationship between absorption and molar extinction coefficient leads to

$$\int \frac{\varepsilon(\upsilon) d\upsilon}{\upsilon} = \int \frac{A(\upsilon) d\upsilon}{cl\upsilon} \cong \frac{1}{cl} \frac{A_{\lambda_{ex}}}{\upsilon_{ex}} FW \tag{7}$$

where $A_{\lambda ex}$ is the absorbance at the excitation wavelength, and FW is the FWHM (Full Width at Half Maximum) of the excitation band. (Because the absorption spectrum does not show a distinct peak, the excitation spectrum (Fig. 9) is used in place of the

absorption spectrum to estimate the width.) The area under the peak is then found by using the absorbance at the excitation wavelength multiplied by the FW of the excitation band.

With the substitution of Eq (7) into Eq (2), the concentration of the fluorophore can finally be found using following equation.

$$c = \frac{2.88 \times 10^{-9} n^2 \left\langle \upsilon^{-3} \right\rangle^{-1} A_{\lambda_{ex}} FW}{l \cdot k_r \cdot \upsilon_{ex}} \tag{8}$$

Table 2 contains the parameters needed to calculate the concentrations at different excitation wavelengths and the concentrations so determined. The results in Table 2 show that the concentration of fluorophore decreases as the excitation wavelength increases. For chromophores absorbing at 400 nm, the mole fraction of chromophores in $[N_{ip311}^+][Tf_2N^-]$ is about 3 ppm, and 15 ppm for $[Pr_{31}^+][Tf_2N^-]$. With this level of impurities a solvent would be considered to be very pure for most applications. But for an fluorescence experiments, this level of impurities is enough to cause problems such as long absorption tail and excitation wavelength dependent emission spectra.

The same calculation was also performed for $[Pr_{31}^+][Tf_2N^-]$ for all three excitation wavelengths, and Tables 3 & 4 include all the relevant quantities for these calculation. The average concentration of fluorophore in $[N_{ip311}^+][Tf_2N^-]$ is 10 μM, and 70 μM for $[Pr_{31}^+][Tf_2N^-]$. This difference is consistent with their emission spectra; the intensity of $[Pr_{31}^+][Tf_2N^-]$ emission is much higher than that of $[N_{ip311}^+][Tf_2N^-]$ when excited at the same wavelength.

Table 1: Parameters* Needed to Calculate Quantum Yield of $[N_{ip311}^+][Tf_2N^-]$ at

λ_{ex} = 360, 400, and 440 nm

λ_{ex} (nm)	I_R	I_S	A_R	A_S	Quantum Yield
360	5.66×10^{6}	1.92×10^{6}	4.59×10^{-3}	3.22×10^{-2}	1.8×10^{-2} $\pm 3 \times 10^{-3}$
400	2.44×10^{7}	1.21×10^{6}	1.57×10^{-2}	1.58×10^{-2}	1.8×10^{-2} $\pm 2 \times 10^{-4}$
440	2.51×10^{7}	3.37×10^{5}	1.64×10^{-2}	9.42×10^{-3}	1.6×10^{-2} $\pm 5 \times 10^{-4}$

*The refractive index of the reference (n_R) is 1.3265 and of $[N_{ip311}^{+}][Tf_2N^{-}]$ (n_S) is 1.416.

Table 2: Radiative Rate, Nonradiative Rate, and Concentration of the Fluorophore of $[N_{ip311}^{+}][Tf_2N^{-}]$ and the Parameters* Needed to Calculate Concentration at λ_{ex} = 360, 400, and 440 nm

λ_{ex} (nm)	Radiative Rate (s^{-1})	Nonradiative Rate (s^{-1})	$\langle\nu\rangle$ (kcm^{-1})	FW (kcm^{-1})	Concentration (μM)
360	1.8×10^{7} $\pm 3 \times 10^{6}$	9.4×10^{8} $\pm 1 \times 10^{8}$	21.0	5.0	17±3
400	1.8×10^{7} $\pm 9 \times 10^{5}$	9.4×10^{8} $\pm 5 \times 10^{7}$	19.8	5.3	8.6±0.7
440	1.6×10^{7} $\pm 1 \times 10^{6}$	9.5×10^{8} $\pm 7 \times 10^{7}$	18.5	5.2	5.1±0.6

*The lifetime τ of $[N_{ip311}^{+}][Tf_2N^{-}]$ is 1.0 ns.

Table 3: Parameters* Needed to Calculate Quantum Yield of $[Pr_{31}^{+}][Tf_2N^{-}]$ at λ_{ex} = 360, 400, and 440 nm

λ_{ex} (nm)	I_R	I_S	A_R	A_S	Quantum Yield
360	9.09×10^{6}	7.88×10^{6}	6.35×10^{-3}	1.21×10^{-1}	1.9×10^{-2} $\pm 3 \times 10^{-3}$
400	3.91×10^{7}	2.38×10^{6}	4.01×10^{-2}	5.70×10^{-2}	1.6×10^{-2} $\pm 5 \times 10^{-4}$
440	4.17×10^{7}	9.56×10^{5}	4.43×10^{-2}	4.46×10^{-2}	8.3×10^{-3} $\pm 3 \times 10^{-4}$

*The refractive index of the reference (n_R) is 1.3265 and of $[Pr_{31}^{+}][Tf_2N^{-}]$ (n_S) is 1.4199.

Table 4: Radiative Rate, Nonradiative Rate, and Concentration of the Fluorophore of $[Pr_{31}^{+}][Tf_2N^{-}]$ and the Parameters* Needed to Calculate Concentration at λ_{ex} = 360, 400, and 440 nm

λ_{ex} (nm)	Radiative Rate (s^{-1})	Nonradiative Rate (s^{-1})	$\langle\nu\rangle$ (kcm^{-1})	FW (kcm^{-1})	Concentration (μM)
360	1.2×10^{7} $\pm 1 \times 10^{6}$	6.3×10^{8} $\pm 6 \times 10^{7}$	22.7	3.7	100±10
400	1.0×10^{7} $\pm 2 \times 10^{5}$	6.3×10^{8} $\pm 1 \times 10^{7}$	20.6	3.6	50±2
440	5.3×10^{6} $\pm 1 \times 10^{5}$	6×10^{8} $\pm 1 \times 10^{7}$	18.8	3.3	70±2

*The lifetime τ of $[Pr_{31}^{+}][Tf_2N^{-}]$ is 1.5 ns.

5. Dilution Effect

To have a better understanding of the possible origins of the long wavelength absorption and emission, the effect of dilution with acetonitrile (ACN) was studied. Fig. 13 shows data for $[N_{ip311}^{+}][Tf_2N^{-}]$. The highest intensity spectrum in Fig. 13 is that of the neat IL, which has a concentration of 3.41 M. Each sample thereafter is diluted by one half in concentration. A total of eight samples were measured, so that the least concentrated sample is 0.0064 M. Fig. 14 is a plot which shows the relationship between the peak intensity and concentration. As can be seen from Fig. 14, the intensity of the emission band decreases proportionally to the decrease in concentration. The dilution effect with acetonitrile (ACN) was studied with $[Pr_{31}^{+}][Tf_2N^{-}]$ as well (Fig. 15), and the same result was obtained. The intensity of the emission peak of $[Pr_{31}^{+}][Tf_2N^{-}]$ also decreases in proportion to the sample concentration (Fig. 16).

As discussed in the Introduction (Fig. 2), Samanta and coworkers[5,6] have shown that as the concentration of the IL is decreased with dilution, the ratio of the intensity of the long wavelength peak to the short wavelength peak decreases much faster than concentration. They proposed that the neat IL is made from aggregates of ions of many different sizes. When the sample is excited at different wavelengths, different associated species are excited and therefore the emission spectrum shifts as a function of excitation wavelength. This suggestion explains the excitation dependence of neat ILs. But if this explanation is correct, the intensity of the peak should drop dramatically when the sample is diluted. The present dilution experiments on

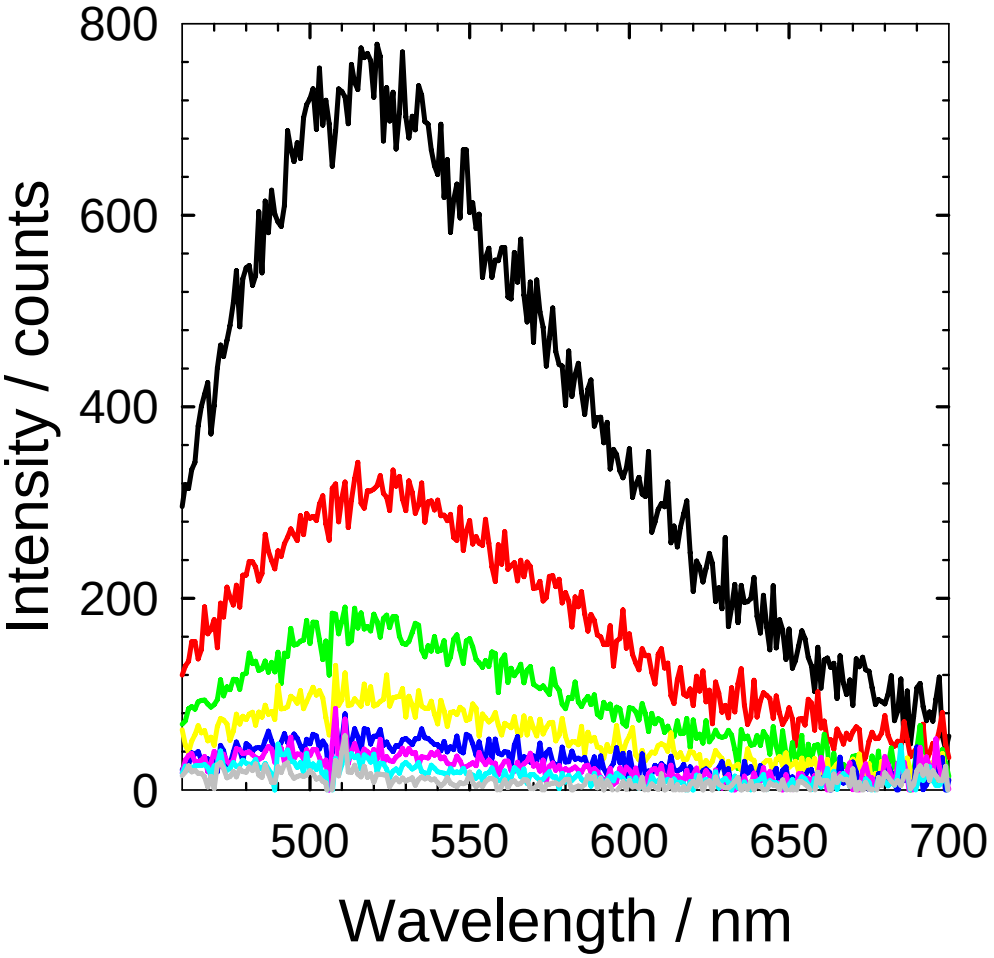

Fig. 13: Effect of dilution with acetonitrile on $[N_{ip311}^{+}][Tf_2N^{-}]$ emission excited at 440 nm. The topmost spectrum is neat IL which has concentration of 3.41 M, then each sample thereafter is diluted by one half in concentration, such that the concentration of last sample is 0.0064 M.

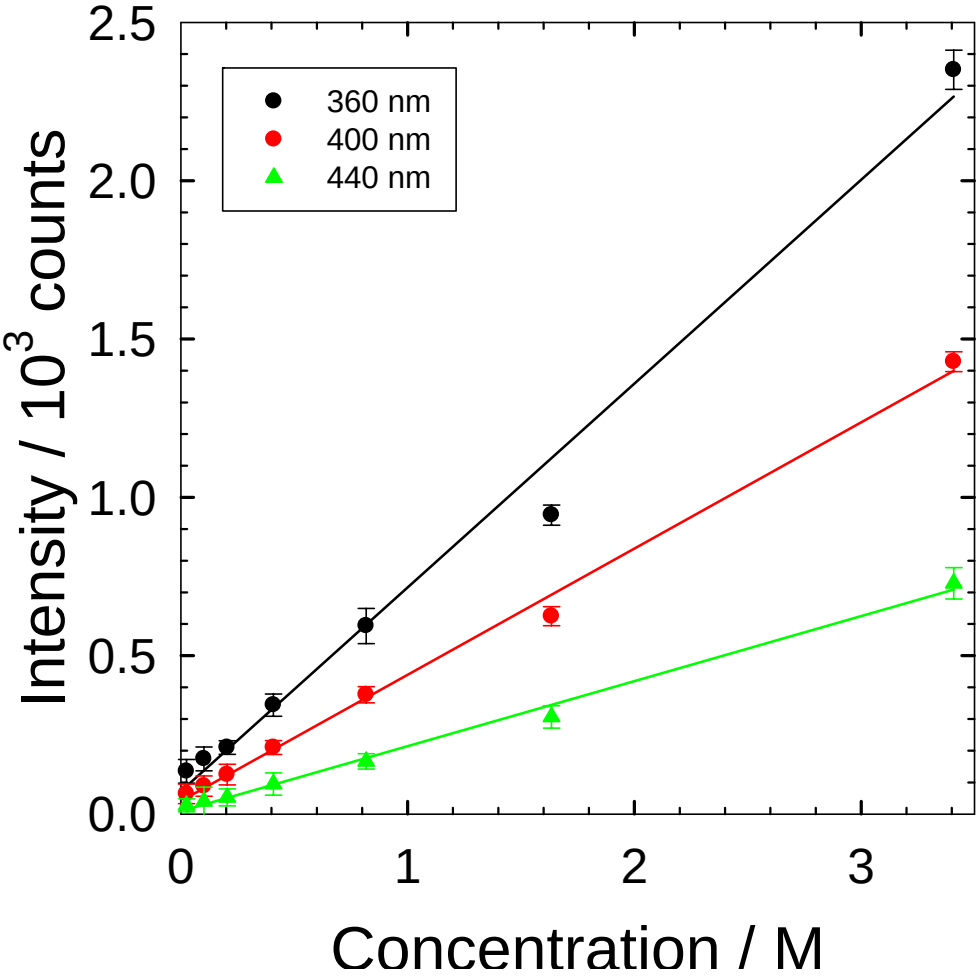

Fig. 14: The plot of peak emission intensity versus the concentration of $[N_{ip311}^{+}][Tf_2N^{-}]$ in acetonitrile diluted samples.

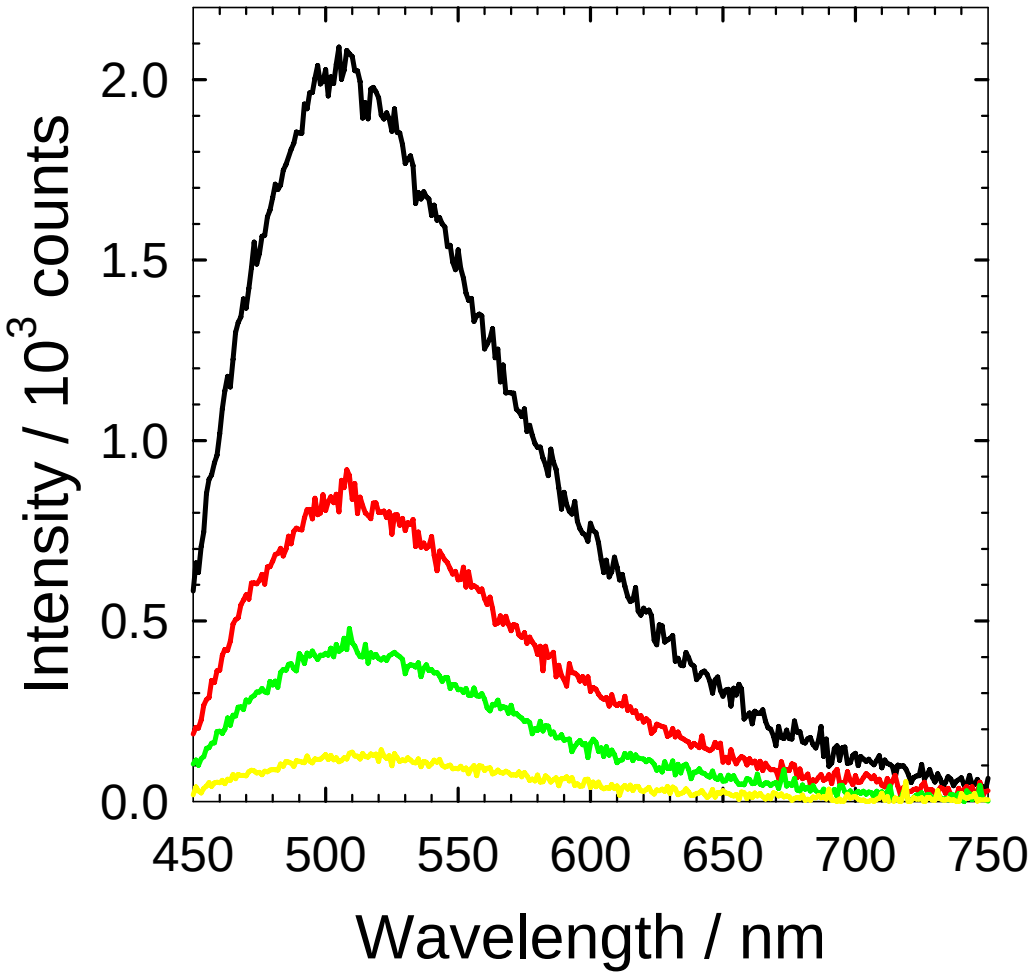

Fig. 15: Effect of dilution with acetonitrile on $[Pr_{31}^{+}][Tf_2N^{-}]$ emission excited at 440 nm. The topmost spectrum is neat IL which has concentration of 3.45 M, then each sample thereafter is diluted by one half in concentration, such that the concentration of last sample is 0.43 M.

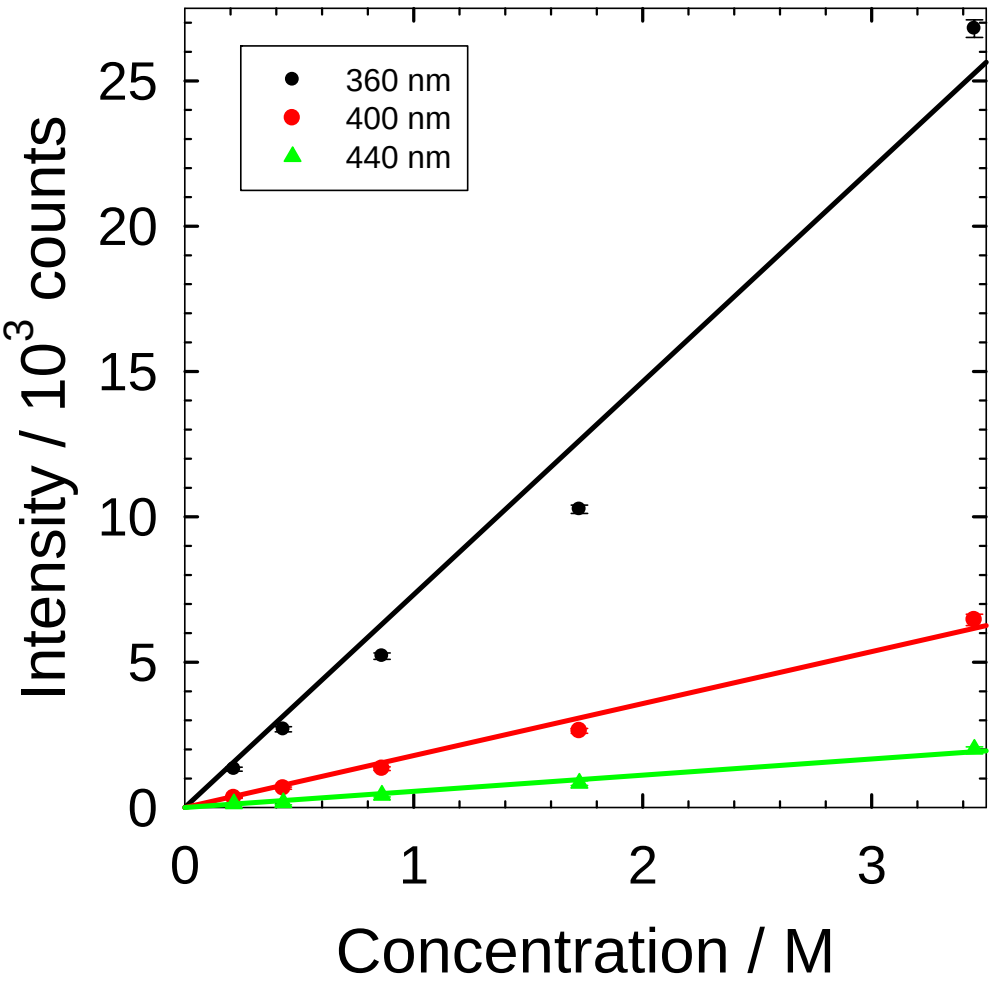

Fig. 16: The plot of peak emission intensity versus the concentration of $[Pr_{31}^{+}][Tf_2N^{-}]$ in acetonitrile diluted samples.

$[N_{ip311}^{+}][Tf_2N^{-}]$ and $[Pr_{31}^{+}][Tf_2N^{-}]$ show that the emission intensity decreases proportionally to the decrease in concentration. This observation is inconsistent with the origin of the fluorescence being ion aggregates.

Discussion

In this paper, we have presented experimental data for two different classes of ILs, ammonium and pyrrolidinium ILs. We have shown that these ILs, like the imidazolium ILs previously studied possess significant absorption and excitation wavelength dependent emission. Even when the isolated ions are not expected to possess electronic transitions at wavelengths larger than 300 nm, significant absorption and emission is observed even at for wavelengths greater than 400 nm. The data suggest two components exist in the samples. One component, whose characteristics are variable in different ionic liquids, gives rise to distinct absorption peaks in the 300 – 400 nm region and strong emission when excited in this region. The second component consists of a long unstructured tail extending out beyond 500 nm in absorption and broad excitation wavelength dependent emission spectra. The features of this emission and the way that it shifts with excitation frequency are similar in all of the ILs that have been studied so far. The origins of this second component are the main interest of the present study.

The first component shows relatively distinct absorption peaks and well defined emission bands but these features vary in different ionic liquids. It seems natural to associate this variable component to specific molecular impurities. The origin of the second component is more puzzling. Based on the fact that all of the ionic liquids show similar emission spectra (Fig. 8), one might assume that this component is intrinsic to the ILs. The broad and unstructured emission spectra and the systematic

shift with excitation frequency argue against this component being a single molecular species. We suggest that a collection of related chromophores with systematically variable properties is responsible for the long wavelength absorption and emission.

Samanta and coworkers proposed that the second component is intrinsic to the ionic liquids based on studies of imidazolium ILs. They conjectured that the long-wavelength emission is due to collections of imidazolium ions and counterions whose collective behavior provides the heterogeneity observed. The authors reached this conclusion mainly because their dilution experiments indicated a decrease in the intensity of the long-wavelength band relative to the short-wavelength monomer band upon dilution. This ion aggregate idea is attractive, but the fact that we observe the intensity of the long-wavelength emission to decrease in proportion to concentration upon dilution without changing character clearly contradicts the idea.

If ion aggregates are not the answer, then what is the origin of the second component? It seems unlikely that the emission is intrinsic to the constituent ions of the IL. The character of emission is similar before and after treatment with activated charcoal, but the intensity of the emission is reduced, which suggests that it is due to some resistant impurity that is at least partially removed by treatment. Also, the fact that $[N_{ip311}^{+}][Tf_2N^{-}]$ and $[Pr_{31}^{+}][Tf_2N^{-}]$ show very different emission intensities suggests impurities that are present in higher levels in $[Pr_{31}^{+}][Tf_2N^{-}]$ compared to $[N_{ip311}^{+}][Tf_2N^{-}]$. The heterogeneous character of the emission clearly rules out any single molecular species, rather it must be some collection of species whose absorption and emission varies systematically with excitation frequency. The absorbance of ILs

at 250 nm is very high (>0.2), but the emission is low when the IL is excited at 250 nm. This observation indicates that the ions do absorb but do not emit light, which suggests that the emission spectra obtained when the IL is excited at other wavelengths which show high emission intensity do not belong to the IL.

The long absorption tail in the visible (Fig. 3) can be explained by the overlapping of a broad distribution of chromophores. As seen from the excitation spectra, the absorption of a selected subset of this distribution shows a typical mirror-image relationship to the emission. Using the bandshapes determined from the excitation spectra and the radiative decay rate, we estimated concentrations. For chromophores absorbing at 400 nm, the concentration were about 8.6 μM (3 ppm) in $[N_{ip311}^{+}][Tf_2N^{-}]$ and 50 μM (15 ppm) in $[Pr_{31}^{+}][Tf_2N^{-}]$. 3 ppm and 15 ppm are low level of impurity for many purposes but it is still too high for fluorescence experiments. With the knowledge of the concentration of chromophores, one can calculated the molar extinction coefficient (ε) using Beer's Law. The result is approximately 3000 cm^{-1} M^{-1} for both ILs. This value identifies the impurities as being moderately strong absorbers – stronger than many simply substituted benzene derivatives. This value along with the wavelength region in which emission occurs suggest that the impurities are likely to be some type of aromatic compounds.

Recently, we examined the excitation wavelength dependence of a number of hard-to-purify conventional solvents such as propylene carbonate (PC) and triacetin. We observed similar behavior in these solvents as in the ILs – a long absorption tail and emission spectra that shift systematically with excitation frequency. These

observations indicate that whatever the impurities are that are responsible for this emission, it is not special to ionic liquids. At this point the identity of this impurity or whether it is the same in different samples is unknown.

Conclusion

We have studied the “intrinsic emission” of ionic liquids. Contrary to previous reports, our results suggest that the emission is not intrinsic but is instead due to some ubiquitous impurity. We conjecture at this point that the emission is due to a collection of different length oligomers of some parent monomer. At present, we have no real idea of what these oligomers might be or why they should be common to all ILs. In order to try to learn more about the identity of these species we are beginning chromatographic experiments. First, we will try to separate the impurity from an ionic liquid using HPLC instrument possessing spectrally resolved UV detection. Once the separation method is developed, HPLC with fluorescence detection and later mass spectral detection will be used to try to establish the identities of the fluorescing impurities.

References:

(1) Wasserscheid, P.; Welton, T. *Ionic Liquids in synthesis*; Wiley-Vch Verlag: Weinheim, 2003.

(2) Tokuda, H.; Hayamizu, K.; Ishii, K.; Susan, A. B. H.; Watanabe, M. *J. Phys. Chem. B* 2004, *108*, 16593-16600.

(3) Tokuda, H.; Hayamizu, K.; Ishii, K.; Susan, A. B. H.; Watanabe, M. *J. Phys. Chem. B* 2005, *109*, 6103-6110.

(4) Seki, S.; Ohno, Y.; Kobayashi, Y.; Miyashiro, H.; Usami, A.; Mita, Y.; Tokuda, H.; Wantanabe, M.; Hayamizu, K.; S., T.; Hattori, M.; Terada, N. *J. Electrochem. soc.* 2007, *154*, A173-A177.

(5) Paul, A.; Mandal, P. K.; Samanta, A. *Chem. Phys. Lett.* 2005, *402*, 375-379.

(6) Paul, A.; Mandal, P. K.; Samanta, A. *J. Phys. Chem. B* 2005, *109*, 9148-9153.

(7) Billard, I.; Moutiers, G.; Labet, A.; Azzi, A. E.; Gaillard, C.; Mariet, C.; Lutzenkirchen, K. *Inorganic Chemistry* 2003, *42*, 1726-1733.

(8) Earle, M.; Gordon, C. M.; Plechkova, N. V.; Seddon, K. R.; Welton, T. *Anal. Chem.* 2007, *79*, 758-764.

(9) Burrell, A. K.; Del Sesto, R. E.; Baker, S. N.; McCleskey, T. M.; Baker, G. A. *Green Chem.* 2007, *9*, 449-454.

(10) Gutkowski, K. I.; Japas, M. L.; Aramendia, P. F. *Chem. Phys. Lett.* 2006, *426*, 329-333.

(11) Arzhantsev, S.; Jin, H.; Baker, G. A.; Maroncelli, M. *J. Phys. Chem. B* 2007, *111*, 4978-4989.

(12) Arzhantsev, S.; Jin, H.; Baker, G. A.; Ito, N.; Maroncelli, M. *Femtochemistry VII, Ultrafast Processes in Chemistry, Physics, and Biology* 2006, 225-234.

(13) Arzhantsev, S.; Jin, H.; Ito, N.; Maroncelli, M. *Chem. Phys. Lett.* 2005, *417*.

(14) Ito, N.; Arzhantsev, S.; Maroncelli, M. *Chem. Phys. Lett.* 2004, *396*, 83-91.

(15) Ito, N.; Arzhantsev, S.; Heitz, M.; Maroncelli, M. *J. Phys. Chem. B* 2004, *108*, 5771-5777.

(16) Arzhantsev, S.; Ito, N.; Heitz, M.; Maroncelli, M. *Chem. Phys. Lett.* 2003, *381*, 278-286.

(17) Heitz, M.; Maroncelli, M. *J. Phys. Chem. A* 1997, *101*, 5852-5868.

(18) Strickler, S. J.; Berg, R. A. *J. Chem. Phys* 1962, *37*, 814-822.

(19) Lewis, J. E.; Maroncelli, M. *Chem. Phys. Lett.* 1998, *282*, 197-203.